Analyst

ROYAL SOCIETY OF CHEMISTRY

PAPER

View Article Online
View Journal | View Issue

Cite this: *Analyst*, 2020, **145**, 5532

Electro-hydrodynamic extraction of DNA from mixtures of DNA and bovine serum albumin†

Benjamin E. Valley, Anne D. Crowell, Jason E. Butler and Anthony J. C. Ladd *

We report separation of genomic DNA (48 kbp) from bovine serum albumin (BSA) by the electro-hydrodynamic coupling between a pressure-driven flow and a parallel electric field. Electro-hydrodynamic extraction exploits this coupling to trap DNA molecules at the entrance of a microfluidic contraction channel, while allowing proteins and salts to be flushed from the device. Samples (10 μL) containing λ-DNA (1 ng) and BSA (0.3 mg) were injected directly into the device and convected to the contraction channel entrance by a flowing buffer solution. The DNA remains trapped in this region essentially indefinitely, while proteins and salts are eluted. The effectiveness of the concept has been assessed by fluorescence measurements of DNA and BSA concentrations. Electro-hydrodynamic extraction in a single-stage device was found to enhance the concentration of DNA 40-fold, while reducing the BSA concentration by four orders of magnitude. The relative concentrations of DNA to BSA at the contraction channel entrance can be as large as 1.5 : 1, corresponding to an A260/280 ratio of 1.9. The maximum yield of DNA from a salt-free solution is 50%, while salted (150 mM) solutions have a lower yield (38%).

Received 12th May 2020,
Accepted 23rd June 2020

DOI: 10.1039/d0an00961j

rsc.li/analyst

1. Introduction

Analysis of genetic material is important to health care, food safety, forensic science, and other industries.[1] While many protocols exist for high purity extracts, most involve lengthy procedures, harsh reagents, and constant intervention.[2] In order to overcome these limitations, DNA extraction has become an area of interest to microfluidic researchers.[3] Microfluidics is assumed to be the key to miniaturization and automation of genetic analysis within a micro total analysis system (μTAS).[4] However, it is first necessary to prepare the sample for analysis by purifying the solution of proteins and cations, which act as PCR inhibitors.[5,6]

Proposed microfluidic platforms for DNA extraction include those based on isotacophoresis, bifurcated field-flow fractionation, and ion selective membranes.[6–9] However, these platforms include buffer gradients, intricate channel geometries, and embedded membranes, which complicate fabrication and operation of the device. Recently, a number of groups have investigated a different class of devices, which rely on transverse migration of DNA to effect the separation.[3,10–17] In contrast to traditional field-flow fractionation, here the transverse motion is driven by a non-linear coupling of axial fields. Although the devices are quite similar in design, we can distinguish between different physical mechanisms causing the transverse migration: electro-inertial,[3,18,19] electro-hydrodynamic[10–14] and electro-viscoelastic.[15–17] The active mechanism in a particular experiment depends on the type of particle and the buffer solution properties.

Electro-inertial migration (EIM) occurs when an electric field causes a charged particle to lead or lag behind the fluid motion, producing a Saffman force[20] towards the wall (lead) or towards the center (lag). There are a growing number of microfluidic applications of EIM,[21] but it cannot lead to particle trapping,[11,15] which requires both migration towards the wall and electrophoresis counter to the flow (lag). Trapping of DNA was first observed[11,15] in somewhat similar devices but under rather different conditions. In one case the fluid was Newtonian, the device relatively large (100 μm) and the shear rates moderate (5–50 s^{-1}).[11] Theory suggests that the transverse migration follows from the stretching and orientation of the DNA by the shear; the intrinsically anisotropic electrophoretic mobility of a non-spherical particle then gives rise to a component of the electrophoretic velocity perpendicular to the field.[22–24] We have chosen to call this effect electro-hydrodynamic migration (EHM). Transverse migration is also observed in viscoelastic fluids (electro-viscoelastic migration or EVM), typically in smaller (<10 μm) channels with significantly higher shear rates (up to 500 s^{-1}).[15] In this case, normal stresses on the polymer create the transverse force on the DNA molecules.[25] However, normal stresses are not necessary for

Department of Chemical Engineering, University of Florida, Gainesville, FL, USA. E-mail: tladd@che.ufl.edu; Tel: +1 (352) 392-6509

†Electronic supplementary information (ESI) available: Additional details of Experimental methods. See DOI: 10.1039/D0AN00961J

EHM,[13] so EHM and EVM are distinct phenomena. With a growing understanding of the underlying mechanisms, chip design, solution chemistry, and operating conditions can be optimized for different applications.

In this work we apply electro-hydrodynamic migration (EHM) to the extraction of DNA from physiological concentrations of BSA. The trapping of DNA by EHM or EVM is particularly advantageous for extraction, because it can potentially permit a complete separation of DNA from proteins and salts in a single stage. Here, we address several issues relevant to the use of EHM as a microfluidic purification technology. First, we have considered the injection of a concentrated sample of DNA (0.1 ng μL^{-1}) into a flowing buffer solution, rather than premixing the sample with the buffer in much lower concentrations (as small as 1 fg μL^{-1}).[12] To include a sample injection port, we have fabricated simple but durable devices from PMMA sheets. Second, although we know that genomic DNA can be trapped by EHM,[11] we do not know how trapping is affected by the large concentrations of proteins found in a typical lysate. Here, injected samples containing small amounts of DNA (1 ng) were contaminated with a large excess of BSA (0.3 mg) to investigate if the DNA remains trapped while the protein is flushed. Lysates also contain salts and other ions, which suppress migration[13] and inhibit PCR. In premixed buffer solutions, salt concentrations in excess of 50 mM were sufficient to prevent migration and trapping. In the present experiments only the sample contains salt, so that it is immediately diluted by the (salt-free) buffer solution. We investigate if there can be trapping of DNA from samples containing physiologically relevant (150 mM) salt concentrations. Finally, and most importantly, we wish to ensure that the protein concentration is sufficiently small that the sample can be considered to be pure DNA, which is typically correlated with A260/280 ratios in excess of 1.8.

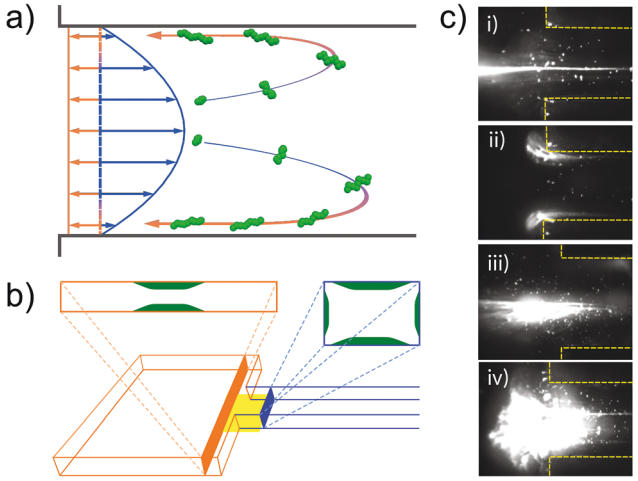

Fig. 1 Extraction of DNA by electro-hydrodynamic migration. (a) DNA molecules (green) mixed with BSA (not shown) enter the contraction channel due to the parabolic flow (blue arrows), with a maximum velocity ν_0. The electric field induces an opposing electrophoretic velocity ν_e (orange arrows), which is an order of magnitude less than the convective velocity; in these experiments ν_e ranges from $-0.015\nu_0$ to $-0.075\nu_0$. The negative sign for the electrophoretic velocity indicates that it opposes the convective flow. DNA molecules migrate toward the channel walls as indicated by the blue-to-orange arrows and return to the entrance of the channel (orange arrows) because the electrophoretic velocity very near the wall exceeds the fluid velocity. (b) Solutions containing mixtures of DNA and BSA are convected from the upstream region (orange) into the contraction channel (blue). The distribution of DNA (green) within cross sections of the device is highly non uniform (orange and blue rectangles). (c) Fluorescence images of DNA concentration at the entrance to the contraction channel (indicated by the yellow outlines); the channel is approximately 350 μm wide and 150 μmm deep. The location of the viewing window within the device is indicated by the yellow rectangle in Fig. 1b. The centerline fluid velocity and opposing electrophoretic velocity were (in mm s^{-1}): (i) 4.4 and −0.09, (ii) 4.4 and −0.12, (iii) 8.8 and −0.12, and (iv) 11 and −0.15.

2. Principles of electro-hydrodynamic extraction

Electro-hydrodynamic extraction adds a new separating mechanism – the flexibility of the chain – which is not present in either EIM or EVM. A polyelectrolyte, such as DNA, is isotropically distributed on scales longer than the Kuhn length (100 nm) and, in the absence of flow, λ-DNA (48 kbp) is distributed within a small sphere less than 1 micron in radius. However, under shear it extends to at least 70% of its contour length[26] or about 15 μm. Importantly the long axis rotates in the flow-gradient plane to lie at a small angle to the field lines.[27,28] Typical orientations of a polymer in a parabolic flow field are indicated by the agglomerates of green circles in Fig. 1a.

An elongated charge distribution, for example a charged rod or a stretched polyelectrolyte, has different electrophoretic mobilities perpendicular and parallel to its symmetry axis.[29] If the axis lies at an angle to the electric field direction, this asymmetry in mobility leads to a net motion of the molecule perpendicular to the field lines as well as electrophoresis parallel to them. DNA that is convected through a microcapillary and driven in the opposite direction by electrophoresis becomes highly localized in a thin (10 μm) layer next to the channel walls.[11] The distribution of DNA in the contraction channel is approximated by the sketch of the (blue-framed) cross section in Fig. 1b; the central region of the capillary is essentially devoid of DNA.

When DNA molecules return past the entrance of the contraction capillary (orange region in Fig. 1b) the fields (both shear and electric) drop by an order of magnitude, due to the sudden increase in cross section. Confocal microscopy has shown that DNA upstream of the constriction channel accumulates in a thin sheet near the upper and lower walls of the channel[11] as indicated by the fluorescence images in Fig. 1c. In contrast to DNA, proteins are small and compact. They do not elongate significantly in the flow, so they will not undergo EHM; transverse motion of proteins is purely diffusive and the distribution in the channel remains uniform. Because of the large imbalance of convective and electrophoretic velocities (ν_0

$\sim$ 40–75ν_e), proteins are quickly eluted from the device. It seems likely that DNA and possibly long strands of RNA are the only biomolecules that will exhibit EHM; it is therefore a promising means for microfluidic purification of genomic nucleic acids.

3. Experimental methods

A schematic of the experiment is shown in Fig. 2a; it replicates a design from previous work, which demonstrated accumulation of DNA from pure solutions.[11–13] An additional port has been added to the microfluidic device, so that a sample can be injected directly into the expansion section of the device (orange region in Fig. 1b) rather than having to be premixed with the buffer solution. The new device was fabricated from PMMA rather than glass, using laser ablation to cut the design sketched in Fig. 1b. Brightfield micrographs of portions of the device are shown in Fig. 2b & c.

Tris-EDTA (TE) buffer solution (0.25×) is driven through the device by a height difference between the inlet and outlet reservoirs. Polyvinylpyrrolidone or PVP (66.5 kDa) was added at 0.5% (v/v) to suppress the electroosmostic flow generated by the charge on the PMMA surfaces. Samples (10 μL) containing 0.1 ng μL^{-1} of λ-DNA and 30 mg ml^{-1} of BSA were injected into the expansion channel (orange region in Fig. 1b) and then convected into the contraction channel (blue region in Fig. 1b) by the flowing buffer solution. In some cases, 150 mM salt was added to the sample to study the effect of ionic strength on the separation process.

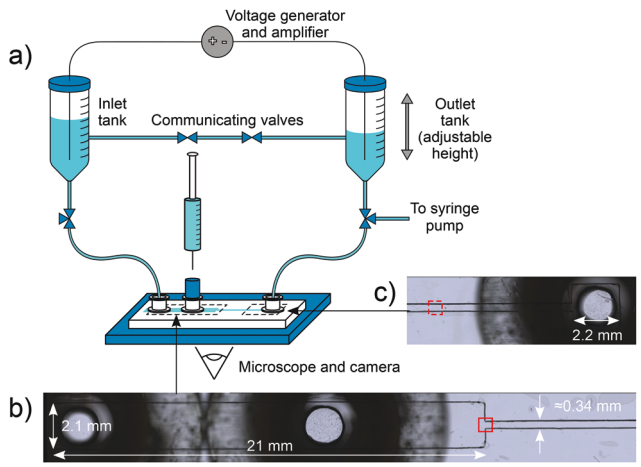

Fig. 2 (a) Schematic of the experimental setup. Samples containing DNA–BSA mixtures are injected directly into the device and convected towards the outlet reservoir by the higher pressure at the inlet port. An electric field is generated by applying a voltage to the fluid in the reservoirs. The dashed lines indicate the location of the brightfield images. (b) Brightfield micrograph of the inlet portion of the device; the dimensions are indicated on the figure. The circles (from left to right) are the solution inlet and sample injection ports. The red solid square marks the location where the accumulation of DNA (Fig. 3) and the elution of BSA (Fig. 4) were measured. (c) Brightfield micrograph of the outlet portion of the device; the width of the channel is about 340 μm. The red dashed square marks the location where the elution of DNA (Fig. 5) was measured.

Extraction experiments were performed as follows. First, fluid levels were equilibrated by opening communicating valves located on the line connecting the two reservoirs (Fig. 2a), to ensure there was no-flow within the channel prior to the experiment. Once equilibrium was achieved, the communicating valves were closed. Next, a 10 μL sample was injected directly into the expansion section of the device as illustrated in Fig. 2a. After sample injection, an electric field and pressure-driven flow were imposed; calibration experiments (ESI†) were used to connect the desired flow rate and electrophoretic velocity of DNA to the height difference and voltage drop between the reservoirs. Between each experiment, the channel was rinsed for five minutes by redirecting the flow to a syringe pump (Fig. 2a), which draws fresh buffer solution from the inlet tank through the channel at a flow rate of 6.9 mL h^{-1}.

Fluorescent images acquired during the extraction process were used to quantify DNA and BSA concentrations at the entrance and near the exit of the contraction channel (red squares in Fig. 2b & c). DNA was tagged with YOYO-3 at a ratio of four base pairs to one dye molecule, while 2.5% (w/w) of the BSA was labeled with fluorescein (FITC). YOYO-3 emits red light (612/631 nm excitation/emission) while FITC emits green light (494/520 nm), which can be measured independently using green and blue excitation filters.

DNA accumulation kinetics were measured at the entrance to the contraction channel (solid red square in Fig. 2b). Images of samples, illuminated briefly to minimize photobleaching of the YOYO-3 fluorophore, were taken at four evenly spaced intervals using the green excitation filter. An 8× neutral density filter, with an exposure time of 200 ms and a camera gain setting of 30, were used to ensure accurate measurement of high concentrations of DNA without saturating the individual pixels. Only DNA was fluorescently tagged in these experiments, to avoid interference from light emitted by FITC-BSA, which is measurable even with the green excitation filter.

BSA elution rates were measured in a similar fashion to DNA accumulation kinetics. Images illuminated by the blue excitation filter were taken with different neutral density filters, to capture the full range of BSA concentrations. High concentration BSA was imaged by illuminating the device every 30 seconds for 20 minutes using the 8× neutral density filter. In subsequent experiments, trace concentrations of BSA were imaged every five minutes without any neutral density filtering; the less frequent illumination reduces photobleaching of the fluorophore.

The amount of DNA that can be extracted from an injected DNA–BSA mixture was quantified by turning off the electric field after a specified time (20–40 minutes), releasing the accumulated DNA from the device. The eluting DNA was imaged as it exited the contraction channel (dashed red square in Fig. 2c). The shutter was left open for the full duration of the experiment to photobleach any DNA that was adsorbed on the viewing window during the extraction. The released DNA was

illuminated only very briefly as it passed over the viewing window. The total mass of DNA trapped during the extraction was estimated from the time integral of the concentration profile $C(t)$,

$$M_{\text{out}} \approx Q \int_0^{\tau} C(t)\mathrm{d}t, \quad (1)$$

where Q is the mass flow rate and $\tau = 120$ s is the time required to elute all of the DNA from the device.[13]

Further details of the device fabrication, the solution and sample preparation, and the calibrations converting fluorescence intensity to concentration are given in the ESI.†

4. Results and discussion

Rapid accumulation of DNA at the entrance to the contraction channel (solid red square in Fig. 2b) was observed for a range of pressure and voltage differences across the device, as indicated by the images in Fig. 1c. We use the fluid centerline velocity (v_0) and the electrophoretic velocity of DNA (v_e) to characterize the pressure and voltage drops across the device. We report the electrophoretic velocity with a negative sign to emphasize that it opposes the fluid motion. Fluorescence images show that the DNA remains localized (or trapped) in this region for long periods of time. Quantitative measurements of DNA trapping at the entrance of the contraction channel are shown in Fig. 3.

To connect to previous work we have measured the trapping of DNA from samples without BSA (open circles in Fig. 3).[11,12] Here we have injected much more concentrated samples (15–600 fold) into roughly cut acrylic devices (Fig. S1b†), as opposed to precise (but expensive) devices made commercially from silica.[11] However, the present devices and protocols seem equally efficient at trapping DNA. The peak concentration (3–4 ng μL^{-1}) compares favorably with previous observations of peak concentrations around 1 ng μL^{-1} in silica devices.[12] DNA trapping is maximized at similar ratios of flow and electrophoretic velocities, independent of cross-sectional size and shape.[12] DNA concentrations in a mixture of DNA and BSA reach almost the same maximum value as pure DNA samples, after only slightly longer processing times (20 *versus* 15 minutes). We can deduce that BSA has only a minimal effect on the accumulation of DNA.

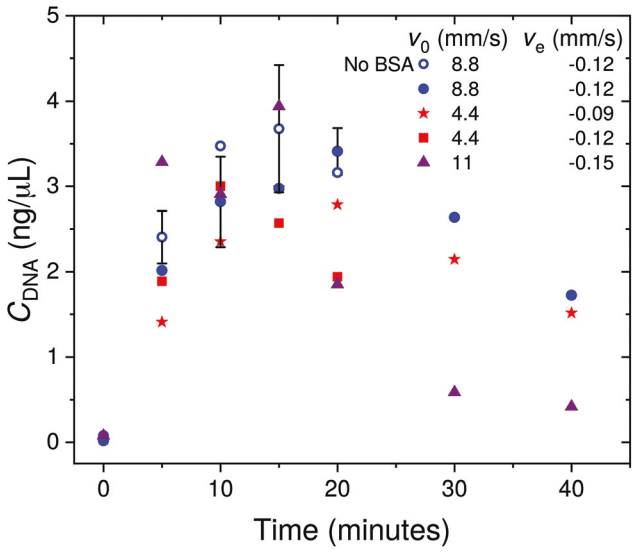

Fig. 3 DNA accumulation at the entrance to the contraction channel (solid red square in Fig. 2b). DNA concentrations, averaged over the viewing window, after injecting a 10 μL sample containing 0.1 ng μL^{-1} DNA and 30 mg mL^{-1} BSA. The open circles indicate samples without BSA. The error bars are one standard deviation (n = 3).

In previous work, devices were pre-coated with PVP in addition to the dynamic coating in the buffer solution. Here only the dynamic coating was used, suggesting that the pre-coating is not essential in preventing electroosmosis. Eliminating PVP entirely does not prevent EHM, but the concentration of trapped DNA was reduced by an order of magnitude. The decrease in trapping efficiency stems from the (positive) electroosmotic velocity of the uncoated acrylic surfaces, which acts against the (negative) electrophoretic velocity of the DNA. EHM itself is independent of electroosmosis, but trapping is not since it depends on the (net) axial velocity of DNA near the channel walls.

Results for different flow and electrophoretic velocities (Fig. 3) are similar, with peak concentrations of 3–4 ng μL^{-1} 15–20 minutes after injection. This represents a 40-fold increase over the initial concentration of DNA injected into the device (0.1 ng μL^{-1}). Previous results suggest that microfluidic devices of comparable size can become saturated with DNA at amounts beyond a tenth of a nanogram.[12] We suspect that not all of the injected DNA can be trapped indefinitely, although this may depend on device dimensions and operating conditions. At the highest electric field (purple triangles in Fig. 3) DNA was drawn back into the channel, upstream of the observation window. The amount of DNA retained within the whole device may be significantly larger than suggested by measurements near the channel entrance; this would be consistent with prior observations of large amounts of DNA trapped upstream of the viewing window when subjected to larger electric fields.[12]

The separation of DNA from BSA was investigated by measuring the decay in concentration of FITC-labeled BSA at the entrance to the contraction channel (red square in Fig. 2b). BSA also has a negative electrophoretic velocity (about one third that of DNA), but because its concentration is uniform across the channel, it is quickly eluted. The high concentration of BSA in the initial sample (30 mg mL^{-1}) produced very large fluorescence signals, which were brought within the dynamic range of the camera by diluting the FITC-BSA 40-fold with unlabeled BSA, and by applying an 8× neutral density filter. The concentration of BSA, shown in Fig. 4a, reaches a peak of 20–22 mg mL^{-1} 1–2 minutes after injection, and then falls off rapidly to something too small to measure (less than 1 mg mL^{-1}) after 3–4 minutes. The BSA concentration at longer times (Fig. 4b) was measured with the 8× neutral density filter

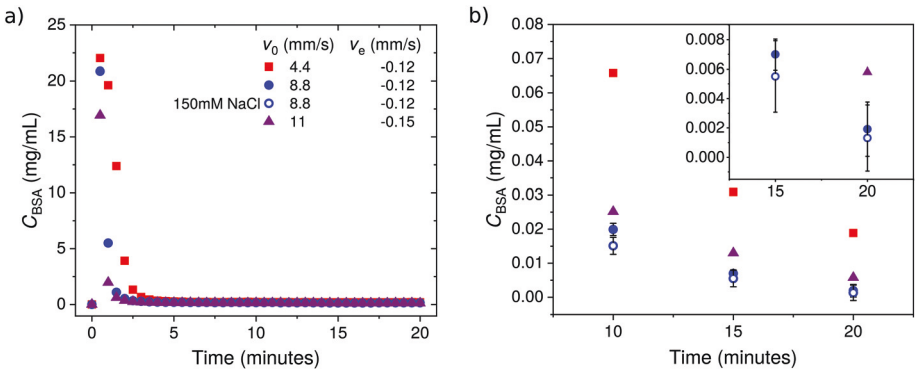

Fig. 4 BSA elution from 10 μL samples containing 0.1 ng μL^{-1} DNA and 30 mg mL^{-1} BSA (2.5% (w/w) FITC-BSA) measured at the contraction channel entrance. (a) High concentration BSA eluting past the viewing window (solid red square in Fig. 2b), measured using 8× neutral density filtering. (b) Trace BSA concentrations eluting at longer times, measured without neutral density filtering. Error bars indicate one standard deviation (n = 3); they are not shown for conditions where only a single experiment was made. The inset figure shows the same results on an expanded scale.

removed to increase the sensitivity of the measurement; after 20 minutes the BSA concentration can be reduced below 0.01 mg mL^{-1}. The optimal conditions for DNA–BSA separations in these experiments were ν_0 = 8.8 mm s^{-1} and ν_e = −0.12 mm s^{-1}, in which case the concentration can be reduced to approximately 2 μg mL^{-1} as indicated in the inset figure. DNA was fluorescently tagged in all the experiments reported in Fig. 4, so that DNA trapping could be verified after BSA elution was complete. Under the blue excitation filter, DNA fluorescence does not interfere with the FITC-BSA signal.

The amount of DNA retained in the microfluidic device after 20–40 minutes of extraction was estimated from the concentration pulse passing the channel exit (dashed red square in Fig. 2c) when trapped DNA was flushed from the device (Fig. 5a). The flush is initiated by turning off the electric field, whereupon the trapped DNA is released and flows out of the device within about 2 minutes. Typical concentration profiles at the channel exit are shown in Fig. 5a. A concentration pulse passes through the viewing window soon after the electric field is turned off. Subsequently the concentration decays to zero, indicating that all the DNA has left the device. The total amount of DNA trapped during the extraction can be estimated by integrating the concentration profile (eqn (1)); results are shown in Fig. 5b.

The maximum yield of purified DNA was obtained after 20 minutes of extraction (orange bars), when up to 50% of the injected DNA can be recovered. The yield is not sensitive to the exact fluid and electrophoretic velocities, varying between 34% and 50% for the conditions investigated in this work. The DNA flushed from the device is of high purity, containing only trace concentrations of BSA, similar to those shown in Fig. 4b. This was confirmed by experiments with FITC-labeled BSA under the blue excitation filter; no measurable fluorescent intensity was observed in this case.

DNA extraction from samples containing BSA salted with 150 mM NaCl was used to better simulate physiological conditions characteristic of blood serum samples. Maximum yields for salted samples (blue bars, Fig. 5b) are reduced in comparison to salt-free samples; in the optimal case (ν_0 = 8.8 mm s^{-1}, ν_e = −0.12 mm s^{-1}) by only 25%. Previous experiments showed that salt concentrations in the buffer solution above 50 mM were sufficient to suppress EHM almost

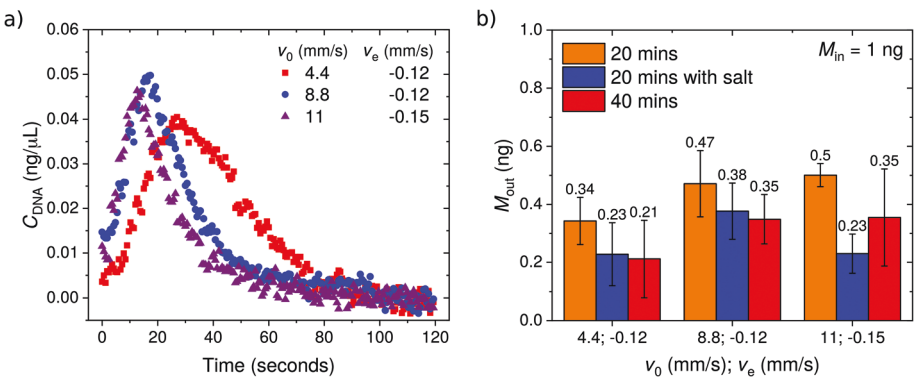

Fig. 5 Mass of trapped DNA from injected samples containing 1 ng DNA and 0.3 mg BSA. (a) Concentrations of DNA at the outlet (dashed red square in Fig. 2c) measured following the release of the trap (by setting the voltage drop to zero). (b) Mass of DNA trapped in the device after 20 minutes (orange bars), 20 minutes with salted samples (blue bars), and 40 minutes (red bars). Error bars indicate one standard deviation (n = 3).

entirely.[13] Here, although the salt concentration in the injected sample was higher (150 mM), it is rapidly diluted by mixing with the (salt-free) buffer solution.

Extraction times of 40 minutes were used to determine if the decrease in DNA concentration at the contraction channel entrance was due to DNA escaping from the device. DNA yields after a 40-minute extraction (red bars in Fig. 5b) were found to vary significantly between experiments, and were on average lower than those from a 20 minutes extraction. The reduction in the average yield suggests that some DNA is leaking from the device, although it is less than suggested by the results in Fig. 3. The large fluctuations in yield at longer times suggest that the trapping may be sensitive to the sample injection which varies considerably from experiment to experiment.

5. Conclusions

We have demonstrated for the first time an EHM-based extraction, enrichment, and detection of nucleic acids from mixtures containing large amounts of bovine serum albumin. After 15–20 minutes, a fraction of the injected DNA becomes trapped within a small portion of the device, where it can be imaged or subjected to on-chip analysis. Our results verify that three requirements of a practical microfluidic extraction method have been met. First, that the presence of physiological concentrations of protein does not interfere with the EHM trapping mechanism (Fig. 3). Second, that DNA can be separated from proteins by EHM alone (Fig. 4), with purities comparable to chemical wash kits and yields similar to other microfluidic extractions.[6,7] The measured concentrations of DNA and BSA in the trapping region (solid red square in Fig. 2a) correspond to A260/280 ratios in the range 1.8–1.9. Third, in conjunction with PCR amplification, sufficient DNA for conventional genetic analysis and sequencing (~0.5 ng) can be extracted from small amounts of unpurified DNA (1 ng).[7,30]

We emphasize that the extraction described here does not depend on differential electrophoretic velocities of DNA and BSA, or balances between convective and electrophoretic velocities. Instead, EHM-based extraction uses a novel coupling of shear and electric fields to create a strongly inhomogeneous concentration distribution of DNA within the *cross-section* of a micro capillary. In agreement with theoretical predictions, EHM does not operate on proteins; it needs both length and flexibility of the molecular backbone, as well as charge.[22,23] It is therefore highly selective for nucleic acids over proteins.

EHM-based extraction uses no external mass separating agents, except for a dilute coating of neutral polymer to suppress electroosmosis. Dynamic coatings could potentially be avoided altogether by employing permanent EOF-suppressing coatings. DNA can be extracted from microvolume samples (10 μL) in simple, low-cost, acrylic devices. The devices are reusable and durable; the one photographed in Fig. S1a† was used for over 100 injection experiments. EHM-based purification has the potential for integration with other microfluidic operations for complete genomic analysis. It should also be applicable to other nucleic acids of sufficient length (>10^4 bases), including RNA-based virus genomes.

Conflicts of interest

There are no conflicts to declare.

Acknowledgements

This work was supported by the National Science Foundation (Grant No. 1804302). The brightfield micrographs in Fig. 2 were prepared by Ms Julie F. Jameson.

References

1 A. E. Guttmacher, M. E. Porteous and J. D. Mclnerney, *Nat. Rev. Genet.*, 2007, **8**, 151–157.
2 D. Chacon-Cortes and L. R. Griffiths, *J. Biorepos. Sci. Appl. Med.*, 2014, **2014**, 1–9.
3 Y. W. Kim and J. Y. Yoo, *Lab Chip*, 2009, **9**, 1043–1045.
4 A. Aroa, G. Simone, G. B. Salieb-Beugelaar, J. T. Kim and A. Manz, *Anal. Chem.*, 2010, **82**, 4830–4847.
5 W. A. Al-Soud and P. Radstrom, *J. Clin. Microbiol.*, 2001, **39**, 485–493.
6 C. Zhang, G. Sun, S. Senapati and H.-C. Chang, *Lab Chip*, 2019, **19**, 3853–3861.
7 A. Persat, L. A. Marshall and J. G. Santiago, *Anal. Chem.*, 2009, **81**, 9507–9511.
8 Y. Qu, L. A. Marshall and J. G. Santiago, *Anal. Chem.*, 2014, **86**, 7264–7268.
9 W. Ouyang, Z. Li and J. Han, *Anal. Chem.*, 2018, **90**, 11366–11375.
10 M. Arca, J. E. Butler and A. J. C. Ladd, *Soft Matter*, 2015, **11**, 4375–4382.
11 M. Arca, A. J. C. Ladd and J. E. Butler, *Soft Matter*, 2016, **12**, 6975–6984.
12 R. J. Montes, J. E. Butler and A. J. C. Ladd, *Electrophoresis*, 2019, **40**, 437–446.
13 R. J. Montes, A. J. C. Ladd and J. E. Butler, *Biomicrofluidics*, 2019, **13**, 044104.
14 B. Chami, N. Milon, J.-L. F. Rojas, S. Charlot, J.-C. Marrot and A. Bancaud, *Talanta*, 2020, **217**, 121013.
15 H. Ranchon, R. Malbec, V. Picot, A. Boutonnet, P. Terrapanich, P. Joseph, T. Leïchlé and A. Bancaud, *Lab Chip*, 2016, **16**, 1243–1253.
16 D. Li and X. Xuan, *Phys. Rev. Fluids*, 2018, **3**, 074202.
17 M. Serhatlioglu, Z. Isiksacan, M. Özkan, D. Tuncel and C. Elbuken, *Anal. Chem.*, 2020, 6932–6940.
18 Y. Kim, H. Noh, S. Jin and J. Yoo, *Exp. Fluids*, 2011, **51**, 723–730.
19 Y. W. Kim and J. Y. Yoo, *Opt. Laser Eng.*, 2012, **50**, 87–98.
20 P. G. Saffman, *J. Fluid Mech.*, 1965, **22**, 385–400.

21 J. Zhang, S. Yan, D. Yuan, G. Alici, N.-T. Nguyen, M. E. Warkiani and W. Li, *Lab Chip*, 2016, **16**, 10–34.
22 J. E. Butler, O. B. Usta, R. Kekre and A. J. C. Ladd, *Phys. Fluids*, 2007, **19**, 113101.
23 A. J. C. Ladd, *Mol. Phys.*, 2018, **116**, 3121–3133.
24 A. C. Setaro and P. T. Underhill, *Phys. Rev. E*, 2019, **100**, 52501.
25 B. Chami, M. Socol, M. Manghi and A. Bancaud, *Soft Matter*, 2018, **14**, 5069–5079.
26 K. Hirano, T. Iwaki, T. Ishido, Y. Yoshikawa, K. Naruse and K. Yoshikawa, *J. Chem. Phys.*, 2018, **149**, 165101.
27 R. M. Jendrejack, D. C. Schwartz, J. J. de Pablo and M. D. Graham, *J. Chem. Phys.*, 2004, **120**, 2513–2529.
28 R. Prabhakar and J. R. Prakash, *J. Rheol.*, 2006, **50**, 561–593.
29 S. B. Chen and D. L. Koch, *J. Colloid Interface Sci.*, 1996, **180**, 466–477.
30 L. Wu, X. Liu, C. W. Schadt and J. Zhou, *Appl. Environ. Microbiol.*, 2006, **72**, 4931–4941.